



Element and mineral characterization of dust emission from the saline land at Songnen Plain, Northeastern China

CHEN Bing^{1,2,3,*}, KITAGAWA Hiroyuki¹, HU Ke⁴, JIE Dongmei⁵,
YANG Junpeng⁴, LI Jingmin¹

1. Department of Hydrospheric-Atmospheric Sciences, Graduate School of Environmental Studies, Nagoya University, Nagoya 464-8601, Japan. E-mail: bchen@iue.ac.cn

2. Institute of Urban Environment, Chinese Academy of Sciences, Xiamen 361021, China

3. College of Earth Sciences, Jilin University, Changchun 130061, China

4. School of Marine Science, China University of Geosciences, Beijing 100038, China

5. College of Urban and Environmental Sciences, Northeast Normal University, Changchun 130024, China

Received 29 November 2008; revised 24 April 2009; accepted 07 May 2009

Abstract

Recent observations of Asian dust storms show an eastern expansion of the source area to degraded lands, where dust emissions have been little studied. The dust concentrations over the saline land of the western Songnen Plain (SSL), Northeastern China, are circumstantially higher than those from the northwestern Chinese deserts. These concentrations are sensitive to the surface soil conditions and wind velocity on the ground. The dust samples collected during dust storm events on the SSL contain abundant Na, Mg, Al, K, Ca, Fe and Ti, as well as toxic elements such as Cu, V, Zn and Ba. Individual particle analysis reveals that fine saline particles (< 10 µm in diameter) on the saline land, consisting largely of carbonate, halite and sulfate together with lithogenic minerals such as SiO₂ and aluminosilicate, are eventually uplifted during the interval from spring to autumn. The predominantly fine saline particles uplifted from the SSL are likely transported eastward by the winter monsoon circulation and westerlies. Recent degradation of saline lands in Northeastern China would not only increase the frequency of dust storm events in the downwind area, but also might change the chemical composition of the Asian dust emissions.

Key words: element geochemistry; individual particle analysis; Asian dust; dust storm; saline soil; land degradation

DOI: 10.1016/S1001-0742(08)62427-4

Introduction

Dust emissions from arid areas of the world are transported long distances by atmospheric circulation, influencing chemical constituents of the atmosphere (Hwang and Ro, 2006; Wang *et al.*, 2007), modifying cloud formation (Kaufman *et al.*, 2005) and affecting the energy balance of the Earth (Satheesh and Moorthy, 2005). The Asian dust storms, which increase dust concentrations and decrease visibility in the atmosphere, cause serious social and economic problems. Many researchers have focused on the Asian dust emissions from the arid and semiarid areas in Northwestern China, such as the Taklimakan Desert and Gobi Desert. Recent observations of dust storm events indicate that the dust source extends to eastern areas (Kurosaki and Mikami, 2003; Kim, 2008), over which mega-cities spread.

China is susceptible to land degradation on account of climate, geography and considerable population pressure on the land (Liu and Diamond, 2005). Land degradation causes the direct destruction of regional ecosystems and

the potential for emission of soil particles into the atmosphere (Li *et al.*, 2005; Qian *et al.*, 2007; Hoffmann *et al.*, 2008; Zhang *et al.*, 2008), raising environmental and social concerns of a regional and global scale. The Chinese government endeavors to prevent the dust hazard, and now spends more than \$1 billion annually on the cure and management of degraded lands. Decision-makers need confidence that all environment factors provided to them are reliable and robust, as the over- or under-assessment of environmental hazards can cause disastrous economic and social effects.

The Songnen Plain in Northeastern China is considered a representative area for assessing the impacts of recent land degradation on the dust emissions (Chen, 2008). The western part of the Songnen Plain is a wide semi-arid saline land (Songnen saline land; SSL, Fig. 1) on the eastern extension of the Gobi Desert and Inner Mongolian steppe. Climate changes and improper land use have caused the degradation of the fragile grass-cover on the SSL, resulting in an expansion of barren saline land from 2.4×10^4 to 3.2×10^4 km² in the past 50 years and making the saline land one of the fast-growing desertification areas

* Corresponding author. E-mail: bchen@iue.ac.cn

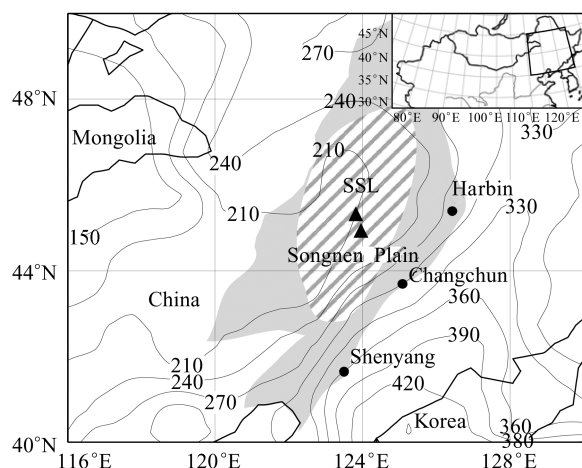


Fig. 1 Map of Songnen saline land (SSL, the pattern area) and sampling sites (triangle) at the nearly central part of the SSL (44.80°N, 123.71°E; 45.27°N, 123.58°E). The contour lines show an annual soil moisture (mm) for 1971–2000 (Fan and van den Dool, 2004).

in Northern China (Li, 2000; Li *et al.*, 2007).

Although some studies on atmospheric dust in North-western China have been carried out (Zhang *et al.*, 2001, 2003), little had been done to investigate the dust emissions from the saline lands in Northeastern China (Chen *et al.*, 2008). In this study, the dust samples were collected from the SSL over two years. Through the major elemental analysis and individual particle analysis, an attempt was made to define the mass loadings and physicochemical characteristics of the dust emissions from the barren saline land in Northeastern China. Our work is the first documentation of the dust emissions from the SSL as a localized source of Asian dust. The documentation on the dust emissions from the saline land should help to assess the environmental and social risks of recently accelerated land degradation.

1 Samples and methods

1.1 Study area

The Songnen Plain has a very flat relief with poor drainage, surrounded by mountains. Thousands tons of minerals are annually carried into the plain by runoff from the surrounding mountains. The groundwater, 1–3 m beneath the ground level, is highly mineralized by sodium bicarbonate (about 5 g/L). The annual precipitation is in the range of 300–600 mm, of which 70% falls in the summer monsoon season between June and September; while the evaporation demand ranges from 1000 to 1500 mm (Ripley *et al.*, 1996). The overall evaporation demand strengthens evapo-transpiration, bringing the solutes dissolved in the groundwater and deep soil up to the surface. The dominant meadow chernozem soil, with organic matter of 3.5%–6% in the surface layer, has developed saline-sodic characteristics (Zhu, 1993). Naturally, the alkalization and salinization progresses with Na_2CO_3 and NaHCO_3 were major sources of soil alkalinity. The over-utilization of the grassland, mainly through overgrazing,

over-mowing and reclamation, results in much faster secondary soil alkalization and salinization process.

The surface soil of the saline land contains a large amount of saline minerals, such as carbonate, halite and sulfate, accompanied by clay minerals (Zheng and Lv, 1995; Li and Zheng, 1997). Droughts can cause salts to accumulate in surface soil, thus frequently leading to surface salt deposits in the dry season (Zheng and Lv, 1995). The major cations are Ca^{2+} and Na^+ , and anion species are CO_3^{2-} , HCO_3^- , SO_4^{2-} and Cl^- . These anions generally account for about 1% of surface soil, ranging up to 10% in some heavily salinized areas (Qiu, 2001). The soil pH is about 8.7 on average, rising as high as 10 in spring, threatening plant growth (Wang and Ripley, 1997). The highly alkali-saline soil facilitates the degradation of the fragile grass-cover.

1.2 Samples

In the period from July 2003 to September 2005, 48 dust samples (total suspended particles) were collected at 4 m above ground level near the central part of the SSL (44.80°N, 123.71°E; 45.27°N, 123.58°E). The samples were collected on 90 mm quartz filters (99.9% retentive for 0.3 μm particles, Pallflex Membrane Filters, Gelman Sciences Inc., USA) mounted on a KB-120 atmospheric sampler. A volumetric air flow-rate of 100 L/min of sampling was maintained for 3–10 h. An air volume of 18–60 m^3 was pumped through the sample filters. Daily-averaged wind velocity at the ground level was observed at a meteorological station on the SSL (45.1°N, 124.2°E). The dust samples collected in different weather conditions and seasons were selected for the elemental and individual particle analyses.

1.3 Elemental analysis

Sixteen samples on quartz filters were completely dissolved in a mixture of concentrated nitric acid, concentrated perchloric acid and concentrated hydrofluoric acid. The concentrations of 14 elements (Na, Mg, Al, K, Ca, Fe, Ti, Mn, Sr, Cu, V, Zn, Ba and B) were determined by inductively coupled plasma with atomic emission spectrometer (ICP-AES, Jarlle-Ash, USA).

1.4 Individual particle analysis

A section of sample filter for thirteen samples was analyzed by scanning electron microscope (SEM) (S-3000N, Hitachi, Japan) coupled to energy-dispersive spectrometer (EDS) (EMAX-500, Horiba, Japan). The elemental abundance and particle size of about 200 particles for each sample were examined at a magnification of 2000. The weight percentages of 24 elements (Na, Mg, Al, Si, S, Cl, K, Ca, Fe, Ba, P, Mn, Sc, Sr, Ti, Ni, Pb, Ag, Mo, Zn, As, Ga, V and Cu) were calculated by a standard ZAF correction method (van Borm and Adams, 1991). We have concluded that the quartz filter did not significantly influence the Si concentration for the determination of elemental composition of particles, because the signal intensity from Si-free particles was under the detection limit (about 0.1% in weight percentage). The particle

size was defined as the average of the long and short dimensions of individual particle.

General cluster analysis on nine major elements (Na, Mg, Al, Si, S, Cl, K, Ca and Fe) was applied for data reduction and interpretation. The particles with similar elemental composition were assigned into a “cluster type”. The number of cluster types was determined using the Akaike’s information criterion (Bondarenko *et al.*, 1994).

2 Results and interpretation

2.1 Dust concentration

The dust concentration varied widely from 20 to 3000 $\mu\text{g}/\text{m}^3$, with an average value of 274 $\mu\text{g}/\text{m}^3$ (Fig. 2). The dust concentration on non-dusty days was estimated to be 100 $\mu\text{g}/\text{m}^3$. The dust concentration increased and significantly high values were observed on 9 March 2004 (2870 $\mu\text{g}/\text{m}^3$), 10 March 2004 (1662 $\mu\text{g}/\text{m}^3$), 13 March 2004 (1125 $\mu\text{g}/\text{m}^3$), 28 March 2005 (781 $\mu\text{g}/\text{m}^3$) and 30 November 2004 (719 $\mu\text{g}/\text{m}^3$). Medium-scale dust storm events were also observed in summer: 17 August 2003 (328 $\mu\text{g}/\text{m}^3$), 20 July 2005 (473 $\mu\text{g}/\text{m}^3$) and 21 August 2005 (390 $\mu\text{g}/\text{m}^3$). Observations in Chinese desert areas have demonstrated concentrations of 270 $\mu\text{g}/\text{m}^3$ in the western Chinese deserts (Zhang *et al.*, 1997, 2001) and 260 $\mu\text{g}/\text{m}^3$ at the southern extreme of the Mu Su Desert in China during the springtime (Zhang *et al.*, 2003). The dust concentration over the SSL was circumstantially higher than those from the main source area of Asian dust emissions.

2.2 Element characterization

According to the data of elemental abundance of the dust samples (Table 1), $(7 \pm 4)\%$ of the total is accounted for by 14 elements. Silicon in lithogenic minerals, as supported by the results of the individual particle analysis, is abundant. The abundances of 7 elements (Na, Mg, Al, K, Ca, Fe and Ti) were generally high for all samples.

Figure 3 shows the temporal variations in the elemental abundance of the dust emissions on the SSL. The sodium abundance was significantly higher in the samples collected in springtime (10 March 2004 and 13 March 2004). It can be expected that the sodium content of

the dust emissions change seasonally. The higher sodium abundance in the dust samples seems to be related to the mineral composition changes of the surface soil, associated with a season-specific pedogenic salt formation in the saline land (Zheng and Lv, 1995).

The enrichment factor (EF) for given element X (normalized to relative to aluminum, Al) of dust relative to that of crust was calculated using equation for elemental dust and crust (Wedepohl, 1995):

$$EF = \frac{\left(\frac{X}{Al}\right)_{\text{dust}}}{\left(\frac{X}{Al}\right)_{\text{crust}}} \quad (1)$$

The element of saline soil origin such as sodium and calcium were enriched by several times (Fig. 4). This confirmed that the saline particles in surface soil were uplifted, at least, in the interval from early spring to late autumn. The wide-range variability of EF for sodium can be explained by the high abundance of sodium in the dust samples of springtime. The enrichment of heavy elements such as Cu, V, Zn and Ba might be related to contamination by toxic materials (Kampa and Castanas, 2008), and/or to natural deposits of brine and groundwater on saline land (Gill *et al.*, 2002).

2.3 Mineral characterization

The cluster analysis identifies 26 cluster types (labeled as C1–C26) based on the weight percentages of nine major elements (Table 2). Due to the limitations of the data handling and the instrument, some other types may have been missed. Six groups (Si-rich, Ca-rich, S-rich, Na-Cl-rich, Fe-rich and zero-count) were categorized from the elemental compositions of 26 cluster types.

The cluster types in the Si-rich group (C1–C10) accounted for 72% of the total particles. They are considered to be composed mainly of SiO_2 and aluminosilicate. Since the particles in the Si-rich group were composed of common lithogenic minerals, it was difficult to infer the mineral species for each type. We noted that the particles of these types contained abundant iron, with the weight percentage ranging up to 8%. This suggests the presence of clay minerals and the potentially spherulitic aggregation of two or more minerals.

The five cluster types in the Ca-rich group (C11–C15), characterized by high calcium and lower sulfur percentages ($< 1.5\%$), accounted for 12% of total particles. The Ca-rich particles were considered to be composed mainly of CaCO_3 . Carbonate materials were abundant in both surface soil and dust samples on the SSL (Chen *et al.*, 2008). The wide scatter of calcium percentages was probably explained by the different extents of aggregation with other minerals.

Five cluster types in the S-rich group (C16–C20) accounted for 7% of the total particles. Four types containing Ca of higher percentage (C16–C19) were suggestive of gypsum ($\text{CaSO}_4 \cdot 2\text{H}_2\text{O}$) or anhydrite (CaSO_4), which are common evaporants in saline lands and/or minerals formed by chemical reaction between calcium carbonate and sulfuric acid. C19 and C20 were notable for higher percentage of Si and Al as well as Na. The Na-containing particles that

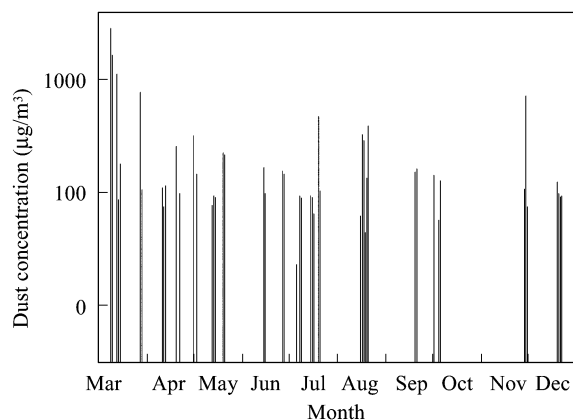


Fig. 2 Dust concentration in the atmosphere over the SSL.

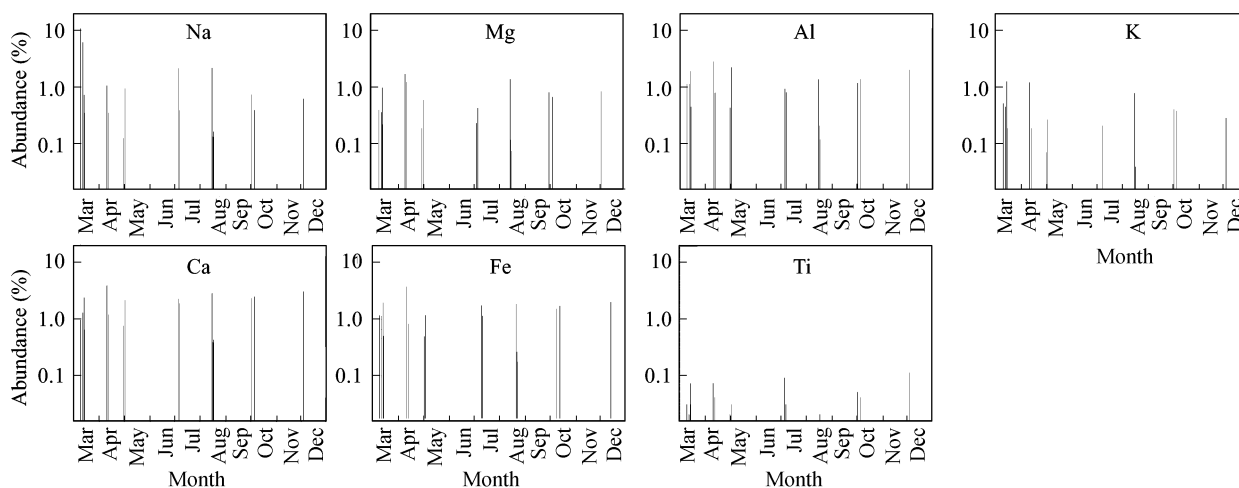


Fig. 3 Temporal variation in the elemental abundance of the dust emissions from the SSL.

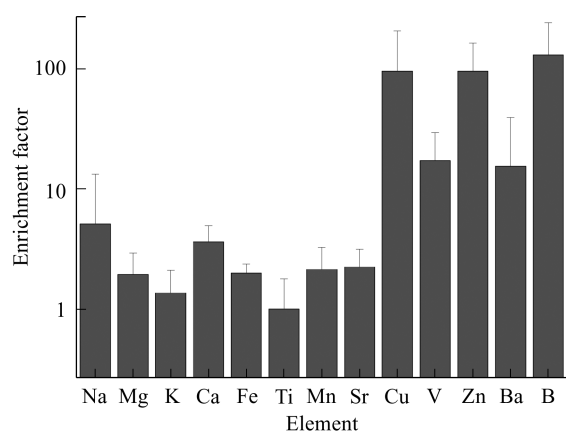


Fig. 4 Enrichment factor (EF) of the elements in the dust emissions from the SSL. EF values are expressed as mean \pm SD.

coexist with sulfur might be naturally occurring mirabilite (Na_2SO_4) deposits of brine or groundwater on saline land (Gill *et al.*, 2002).

Three cluster types of the Na-Cl-rich group (C21–C23), characterized by high sodium and chlorine percentages, and accounted for 6%. The possible mineral was halite (NaCl) which is common in saline soils in the SSL (Zheng and Lv, 1995; Li and Zheng, 1997). The emission of halite particles in arid area has been previously reported (Gillette *et al.*, 2001). C23 was somewhat enriched in sulfur, suggesting the presence of Na_2SO_4 . The relatively high Al and Si percentages in C22 and C23 probably suggest that silicate was internally mixed with NaCl and Na_2SO_4 (Andreae *et al.*, 1986).

A few particles in Fe-rich (C24 and C25) and zero-count (C26) groups were also identified. The Fe-rich particles were 2% of the total particles. Iron oxides or elemental iron from soil were probably encountered. The zero-count type with no detectable elements comprised 35 particles. On the basis of predominance of carbonaceous particles reported in urban atmosphere (Duan *et al.*, 2006), the particles in the zero-count group are likely to be rich in carbon or nitrate.

Table 1 Elemental abundance of the dust samples from the SSL

Sampling date	Dust conc. (g/m^3)	Weight percentage (%)														Contr. (%) [*]
		Na	Mg	Al	K	Ca	Fe	Ti	Mn	Sr	Cu	V	Zn	Ba	B	
6 July 2003	23	2.13	0.22	0.96	nd	2.26	1.61	0.09	nd	nd	0.09	0.04	0.09	0.17	0.04	8
8 July 2003	94	0.38	0.41	0.84	0.21	1.84	1.05	0.03	0.02	0.01	0.01	0.01	0.09	0.03	0.02	5
16 August 2003	61	2.16	1.34	1.41	0.80	2.85	1.66	nd	0.07	0.02	0.11	nd	0.2	0.15	0.05	11
17 August 2003	328	0.13	0.11	0.21	0.04	0.38	0.24	nd	nd	nd	0.01	nd	0.03	0.12	nd	1
18 August 2003	291	0.16	0.07	0.12	nd	0.42	0.16	0.02	nd	nd	0.01	nd	0.02	0.02	0.01	1
02 October 2003	142	0.73	0.78	1.21	0.41	2.32	1.39	0.05	0.04	0.01	0.01	0.05	0.23	0.04	0.02	7
06 October 2003	127	0.39	0.65	1.42	0.39	2.44	1.57	0.04	0.02	0.01	0.02	nd	0.07	0.05	0.02	7
10 March 2004	1661	10.78	0.37	1.16	0.53	0.95	1.08	0.03	0.02	0.01	nd	nd	0.01	0.02	0.01	15
13 March 2004	1125	6.20	0.34	1.16	0.46	1.28	1.03	0.02	0.02	0.01	0.01	nd	0.01	0.02	0.01	11
14 March 2004	87	0.71	0.92	1.97	1.32	2.38	1.79	0.07	0.02	0.01	0.01	0.02	0.03	0.03	0.01	9
15 March 2004	180	0.34	0.21	0.46	0.19	0.63	0.46	0.03	0.01	0.01	0.01	0.02	0.02	0.02	nd	2
11 April 2004	110	1.05	1.65	2.92	1.25	3.97	3.39	0.07	0.07	0.03	0.02	0.05	0.29	0.06	0.03	15
12 April 2004	75	0.61	0.80	2.08	0.29	3.08	1.87	0.11	0.03	0.01	0.08	0.03	0.12	0.05	0.03	9
13 April 2004	115	0.34	1.18	0.82	0.19	1.18	0.74	0.04	0.02	nd	0.01	0.03	0.04	0.03	0.01	5
01 May 2004	319	0.12	0.18	0.44	0.07	0.75	0.45	0.02	0.01	nd	0.01	0.01	0.02	0.01	0.01	2
03 May 2004	146	0.92	0.56	2.32	0.27	2.12	1.07	0.03	0.02	0.02	0.02	nd	0.15	1.17	0.01	9

^{*} Contribution of 14 elements to total.

nd: under the detection limit (about 0.01%) of ICP-AES.

Table 2 Average elemental composition for 26 cluster types of dust samples from the SSL

Cluster type	Particle number	Weight percentage (%)								
		Na	Mg	Al	Si	S	Cl	K	Ca	Fe
Si-rich group (1737 particles, 72% of total particles)										
C1	340	0.0	0.0	0.0	100.0	0.0	0.0	0.0	0.0	0.0
C2	299	0.3	0.1	2.0	95.1	0.8	0.3	0.4	0.6	0.1
C3	267	0.9	0.3	4.0	88.4	1.3	0.6	1.5	1.9	1.0
C4	194	0.9	0.5	9.2	82.6	0.6	0.2	2.9	1.1	1.7
C5	111	2.7	0.5	2.6	80.1	3.4	3.5	1.0	4.5	1.1
C6	144	1.8	0.5	12.6	75.4	0.9	0.5	4.6	1.5	1.9
C7	115	1.1	2.0	9.2	69.0	1.4	1.3	3.1	4.2	7.9
C8	85	4.4	0.4	19.0	67.5	0.6	0.3	2.7	2.7	1.5
C9	129	1.9	3.1	13.7	56.7	1.7	2.4	4.2	7.8	7.2
C10	53	1.3	0.6	14.1	63.4	0.7	0.6	16.3	1.1	1.4
Ca-rich group (298 particles, 12%)										
C11	28	2.2	2.6	3.1	23.2	0.4	1.7	0.3	65.9	0.2
C12	62	3.5	2.0	5.2	40.3	0.9	3.2	1.1	40.2	3.0
C13	63	1.6	1.1	3.2	60.7	2.3	1.9	0.7	26.8	1.4
C14	66	3.7	2.9	11.3	44.5	1.5	5.3	3.6	17.1	5.4
C15	79	0.7	0.9	4.2	74.1	1.3	1.5	1.1	13.9	1.5
S-rich group (161 particles, 6.6%)										
C16	24	0.7	0.4	1.6	22.9	39.3	0.0	3.7	30.3	0.5
C17	52	1.5	1.2	1.8	49.5	25.5	0.1	2.6	16.4	0.8
C18	65	1.6	0.9	1.1	68.4	18.2	0.1	1.1	8.2	0.0
C19	11	4.3	5.5	48.1	2.8	19.5	2.2	2.8	10.6	3.4
C20	9	24.5	0.2	0.8	32.2	35.6	1.4	3.2	1.2	0.3
Na-Cl-rich group (144 particles, 6.0%)										
C21	40	46.5	0.0	1.4	8.0	0.2	43.1	0.0	0.6	0.0
C22	50	28.6	0.2	2.2	33.4	0.8	30.2	0.3	3.9	0.2
C23	54	11.6	0.8	3.7	62.8	2.4	11.9	1.0	4.1	0.9
Fe-rich group (42 particles, 1.7%)										
C24	13	0.1	0.1	1.1	23.6	0.7	0.2	0.1	0.6	70.6
C25	29	1.0	3.8	7.6	53.2	1.2	1.0	1.2	3.7	25.8
Zero-count group (35 particles, 1.5%)										
C26	35									

2.4 Particle size

Figure 5 shows the particle size distribution (PSD) of seven groups. The Si-rich particles were subdivided into two groups based on the different silicon abundance. The PSD of five groups, except for pure SiO₂/aluminosilicate (SiO₂ and aluminosilicate with high Si percentage, C1–C4) and zero-count particles, showed log-normal distributions with a maximum frequency around 5 μm. PSD of pure SiO₂/aluminosilicate group was shifted toward a smaller size, which was close to that of the Chinese loess soils

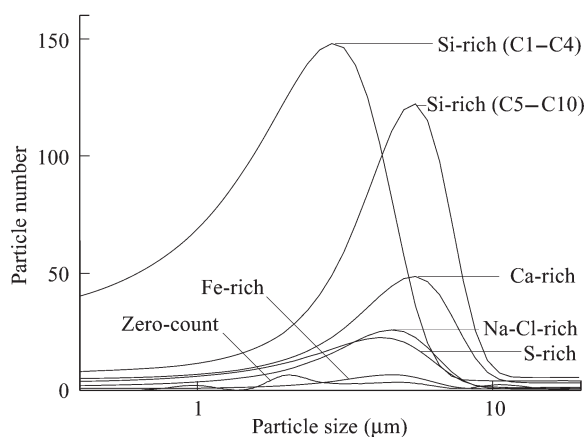


Fig. 5 Particle size distribution (PSD) for seven particle groups. The Si-rich particle group was subdivided based on the different silicon abundances. PSD was fitted using a log-normal distribution curve.

(Kim *et al.*, 2006). The majority of dust particles from the SSL showed somewhat larger sizes than those of the desert origin loess soils (Sun, 2002). This suggests that the pedogenic soils in the SSL were emitted together with the re-generation of the aeolian deposits transported from the northwestern Chinese deserts. The majority of dust particles on the SSL were smaller than 10 μm in size. It is believed that fine particles with size less than 10 μm can be easily uplifted and transported long distances by the Asian monsoon circulation and westerlies (Mikami *et al.*, 2006).

3 Discussion

3.1 Emission of saline particles

The contribution of different particle groups for each sample is shown in Fig. 6. The Ca-rich and Si-rich particles make up rather dominant and constant portions of the total particle number, excluding the sample collected during the heavy dust storm event on 30 November 2004. This sample contained abundant Na-Cl-rich particles thought to be halite. Relatively large concentrations of Na-Cl-rich particles were loaded in springtime and late autumn, when season-specific formation of salt deposits is assumed. This suggests that salt deposits in saline lands during the dry season can change the chemical composition of dust emissions. It was noted that the samples containing high loading of S-rich particles (27 June 2005 and 20 July 2005) were collected under the southerly winds (Fig. 6). The

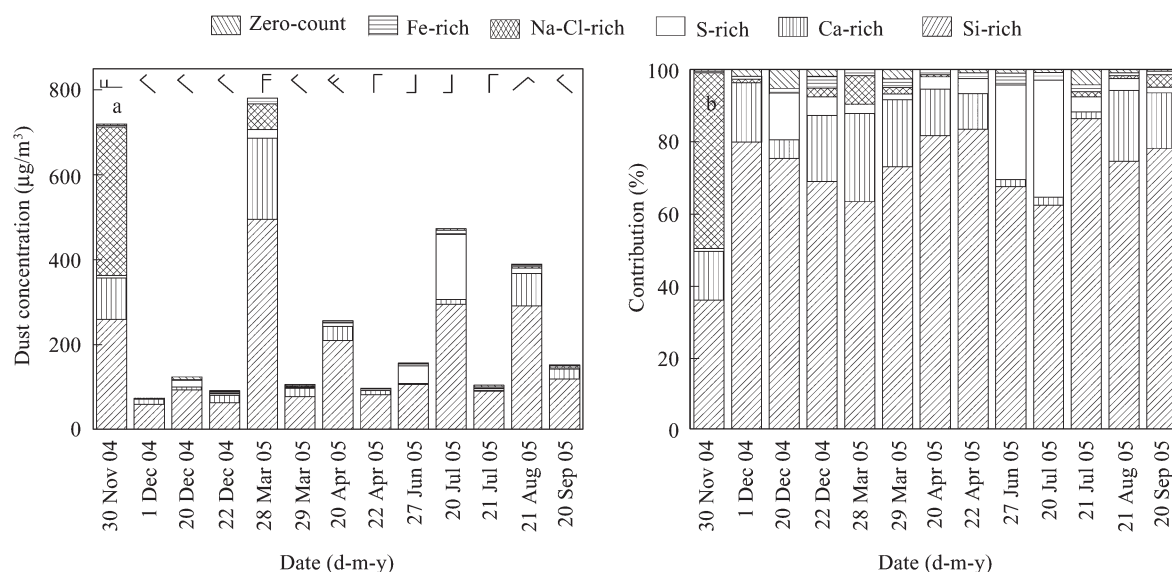


Fig. 6 Concentrations and relative contributions of the different particle groups. The daily averages of direction and strength of surface winds are shown in Fig. 6a.

elemental composition of the dust emissions seems to be sensitive to local meteorological condition. This suggests that, depending on local meteorological and soil conditions on the SSL, saline particles can be easily uplifted into the atmosphere during the interval from spring to autumn. The increased frequency of dust storm events in Northeastern China (Kurosaki and Mikami, 2003; Kim, 2008) was partly related to this enhanced dust emission from the saline lands.

3.2 Enhancing Asian dust emission

The surface wind velocity observed at the meteorological station (45.1°N , 124.2°E), the soil moisture averaged during 1971–2000 (Fan and van den Dool, 2004), the sodium concentration and biomass at the surface soil (Gao *et al.*, 1996) are summarized in Fig. 7. The wind velocity is generally over 4 m/s in springtime. In the Songnen Plain, the soil moisture is lower in springtime and late autumn. The sodium concentration was high in springtime. Except for summer monsoon season, the biomass is as low as about $100 \text{ g}/\text{m}^2$.

The enhanced dust emission in springtime is probably related to the stronger surface winds and the expanded barren saline lands. Soil particles can be uplifted into the atmosphere when the surface wind velocity is over a specific threshold (Grini *et al.*, 2005). The formation of saline particles in soil is enhanced by low soil moisture (Qian *et al.*, 2007). Wind erosion of saline soils is intensified by stronger winds in springtime (Gillette *et al.*, 2001). The increased sodium concentration of dust emissions was presumably from the high sodium concentration in the surface soil. The saline land expansion with less vegetation in springtime might increase the saline dust emissions from the SSL. The increase in the amount of dust emitted would be explained by the combination of these factors. The conditions that favor dust emissions should be sharpened by the recent saline land expansion in Northeastern China.

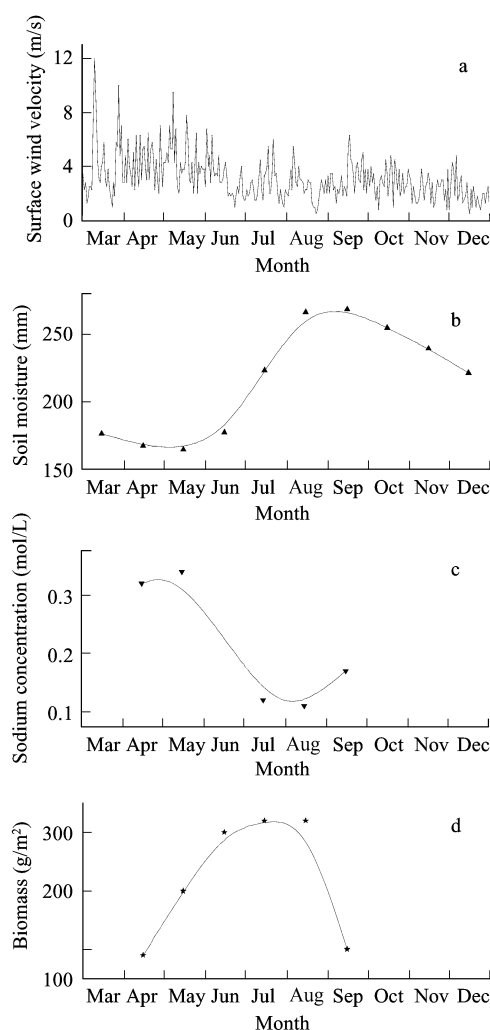


Fig. 7 Potential factors controlling the dust emissions in the SSL. (a) surface wind velocity at a meteorological station on the SSL (45.1°N , 124.2°E); (b) soil moisture during 1971–2000 (Fan and van den Dool, 2004); (c) the sodium concentration (Gao *et al.*, 1996); (d) the biomass at the surface soil (Gao *et al.*, 1996).

The enhanced saline dust emissions should contribute to the generation of dust storm events in the downwind area (Chen *et al.*, 2008). This suggests that the vast degraded lands in Northeastern China enhance Asian dust emissions.

3.3 Effect of saline dust emission

The saline dust emissions from the SSL would be incorporated into the long-lived Asian dust plume and increase dust deposition in downwind area. The saline dust emissions from the SSL contain abundant saline minerals including of halite, calcium carbonate and sulfate. Internal mixing between saline minerals and insoluble silicate, as observed by SEM-EDS, has the potential to change the ability of dust particles to be cloud condensation nuclei and ice nuclei (Andreae *et al.*, 1986), and alter the lifetime and deposition region of the particles (Fan *et al.*, 2004). The high percentage of sodium- and calcium-containing particles in the dust emissions from saline lands can also shift the chemical composition of precipitation. Recent reports show that the precipitation downwind area of the SSL has relatively high salinity and alkalinity (Hu *et al.*, 2001).

The CaCO_3 species is of great interest when we investigate the chemical modification of the Asian dust particles during the long-distance transport (Hwang and Ro, 2006; Wang *et al.*, 2007). This species can react with SO_x and NO_y to produce CaSO_4 and $\text{Ca}(\text{NO}_3)_2$ particles, respectively. The Ca-rich particles containing less sulfur from the SSL could be converted into CaSO_4 or $\text{Ca}(\text{NO}_3)_2$ during transport due to chemical reactions with air pollutants downwind, where mega-cities and industrial areas are located. Indirect evidence for this possibility is provided by the carbonate content of dust samples from a downwind mega-city, which was lower than that of the SSL, even though the dust particles were mostly transported from the SSL (Chen *et al.*, 2008).

The Fe-rich dust emissions from saline lands might be important when we consider the role of Asian dust emissions in the biogeochemical processes of the Northwestern Pacific, where ecosystem productivity is limited by lack of usable minerals (e.g., Zhuang *et al.*, 1992). Saline dust emissions from the dried saline lands, transported by the Asian monsoon circulation and westerlies, would affect the physicochemical processes of the long-lived Asian dust plume.

4 Conclusions

Elemental and individual particle analyses of dust samples collected from the SSL demonstrate that a large amount of fine saline particles is emitted from the saline land in Northeastern China where intensive land degradation is going on. Saline dust emissions from the SSL, consisting predominantly of NaCl , CaCO_3 and CaSO_4 minerals together with lithogenic minerals such as SiO_2 and aluminosilicate, can be distinguished from the long-transported dust from the northwestern Chinese deserts.

The enhanced transport of saline particles likely increases the frequency of dust storm events in downwind

areas, and is a potential explanation for recent eastward expansion of the Asian dust storm events. Saline dust emissions may modify the atmospheric chemistry and physics involved in cloud formation and earth's energy balance, thus potentially playing a role in climate change. Much more attention should be paid to the increase of saline lands in the world associated with intensive land degradation.

Acknowledgments

We thank K. Osada, A. Matsuki and J. Sato of Nagoya University for kind support of SEM-EDS analysis and laboratory works. Thanks are also extending to Dr. X. R. Zhang, Y. Y. Liu, Z. Cao, T. Gu, F. L. Li, L. L. Liu of Jilin University, and Dr. K. T. Zhao, R. Z. Chen of China University of Geosciences for the field sampling in the SSL. China Hongri Corp. had given assistance on field observation. The manuscript has been kindly improved by anonymous reviewers and A. Sage of Kent State University. NCEP Reanalysis Derived data provided by the NOAA/OAR/ESRL PSD, Boulder, Colorado, USA, from their Web site at <http://www.cdc.noaa.gov>. This research was financially supported in a part by Chinese National Key Project of Basic Research (No. G2000048703), and the Grant-in-Aid for Scientific Research (No. 16310008, 18403002) from the Ministry of Education, Culture, Sports, Science and Technology, Japan.

References

- Andreae M O, Charlson R J, Bruynseels F, Storms H, van Grieken R, Maenhaut W, 1986. Internal mixture of sea salt, silicates, and excess sulfate in marine aerosols. *Science*, 232: 1620–1623.
- Bondarenko I, van Malderen H, Treiger B, van Espen P, van Grieken R, 1994. Hierarchical cluster analysis with stopping rules built on Akaike's information criterion for aerosol particle classification based on electron probe X-ray microanalysis. *Chemometrics and Intelligent Laboratory Systems*, 22: 87–95.
- Chen B, 2008. Geochemical characterization of dust emission from the saline land on Songnen Plain, Northeastern China. Ph.D Thesis, Nagoya University, Nagoya.
- Chen B, Kitagawa H, Jie D M, Hu K, Lim J, 2008. Dust transport from Northeastern China inferred from carbon isotopes of atmospheric dust carbonate. *Atmospheric Environment*, 42: 4790–4796.
- Duan F K, He K B, Ma Y L, Yang F M, Yu X C, Cadle S H *et al.*, 2006. Concentration and chemical characteristics of $\text{PM}_{2.5}$ in Beijing, China: 2001–2002. *The Science of Total Environment*, 355: 264–275.
- Fan S M, Horowitz L W, Levy H, Moxim W J, 2004. Impact of air pollution on wet deposition of mineral dust aerosols. *Geophysical Research Letters*, 31: L02104.
- Fan Y, van den Dool H, 2004. Climate prediction center global monthly soil moisture dataset at 0.5° resolution for 1948 to present. *Journal of Geophysical Research*, 109: D10102.
- Gao Q, Yang X S, Yun R, Li C P, 1996. MAGE, a dynamic model of alkaline grassland ecosystems with variable soil characteristics. *Ecological Modelling*, 93: 19–32.
- Gill T E, Gillette D A, Niemeyer T, Winn R T, 2002. Elemental

- geochemistry of wind-erodible playa sediments, Owens Lake, California. *Nuclear Instruments and Methods in Physical Research B*, 189: 209–213.
- Gillette D A, Niemeyer T C, Helm P J, 2001. Supply-limited horizontal sand drift at an ephemerally crusted, unvegetated saline playa. *Journal of Geophysical Research*, 106(D16): 18085–18098.
- Grini A, Myhre G, Zender C S, Isaksen I S A, 2005. Model simulations of dust sources and transport in global atmosphere: Effects of soil erodibility and wind speed variability. *Journal of Geophysical Research*, 110: D02205.
- Hoffmann C, Funk R, Wieland R, Li Y, Sommer M, 2008. Effects of grazing and topography on dust flux and deposition in the Xilingele grassland, Inner Mongolia. *Journal of Arid Environments*, 72: 792–807.
- Hu K, Wu D H, Yang D M, Yang J L, Chen S, 2001. Preliminary study of ecological effects of remote smallsand descending on urban area. *Journal of Changchun University of Science and Technology*, 31(2): 176–180.
- Hwang H J, Ro C U, 2006. Direct observation of nitrate and sulfate formations from mineral dust and sea-salts using low-Z particle electron probe X-ray microanalysis. *Atmospheric Environment*, 40: 3869–3880.
- Kampa M, Castanas E, 2008. Human health effects of air pollution. *Environmental Pollution*, 151: 362–367.
- Kaufman Y J, Koren I, Remer L A, Rosenfeld D, Rudich Y, 2005. The effect of smoke, dust, and pollution aerosol on shallow cloud development over the Atlantic Ocean. *Proceedings of the National Academy of Sciences of the United States of America*, 102: 11207–11212.
- Kim H K, Hwang H J, Ro C U, 2006. Single-particle characterization of soil samples collected at various arid areas of China, using low-Z particle electron probe X-ray microanalysis. *Spectrochimica Acta B*, 61: 393–399.
- Kim J, 2008. Transport routes and source regions of Asian dust observed in Korea during the past 40 years (1965–2004). *Atmospheric Environment*, 42: 4778–4789.
- Kurosaki Y, Mikami M, 2003. Recent frequent dust events and their relation to surface wind in East Asia. *Geophysical Research Letters*, 30: 1736.
- Li J D, Zheng H Y, 1997. The control of alkalized-salinized grasslands in the Songnen Plain and their mechanisms. Beijing: Science Press.
- Li X J, 2000. The alkali-saline land and agricultural sustainable development of the Western Songnen Plain in China. *Scientia Geographica Sinica*, 20(1): 51–55.
- Li F R, Kang L F, Zhang H, Zhao L Y, Shirato Y, Taniyama I, 2005. Changes in intensity of wind erosion at different stages of degradation development in grasslands of Inner Mongolia, China. *Journal of Arid Environments*, 62: 567–585.
- Li X Y, Wang Z M, Song K S, Zhang B, Liu D W, Guo Z X, 2007. Assessment for salinized wasteland expansion and land use change using GIS and remote sensing in the west part of Northeast China. *Environmental Monitoring and Assessment*, 131: 421–437.
- Liu J G, Diamond J, 2005. China's environment in a globalizing world. *Nature*, 435: 1179–1186.
- Mikami M, Shi G Y, Uno I, Yabuki S, Iwasaka Y, Yasui M *et al.*, 2006. Aeolian dust experiment on climate impact: An overview of Japan-China joint project ADEC. *Global and Planetary Change*, 52: 142–172.
- Qian Y B, Wu Z N, Yang Q, Zhang L Y, Wang X Y, 2007. Ground-surface conditions of sand-dust event occurrences in the southern Junggar Basin of Xinjiang, China. *Journal of Arid Environments*, 70: 49–62.
- Qiu S W, 2001. The research on the application techniques about the characteristics, causes and harness of salinization in middle and lower reaches of Huiling River and Tao'er River. *Soil Bulletin*, 32(6): 18–32.
- Ripley E A, Wang R Z, Zhu T C, 1996. The climate of the Songnen plain, Northeast China. *International Journal of Ecology and Environmental Sciences*, 22: 1–22.
- Satheesh S K, Moorthy K K, 2005. Radiative effects of natural aerosols: A review. *Atmospheric Environment*, 39: 2089–2110.
- Sun J M, 2002. Provenance of loess material and formation of loess deposits on the Chinese Loess Plateau. *Earth and Planetary Science Letters*, 203: 845–859.
- Van Borm W A, Adams F C, 1991. A standardless ZAF correction for semi-quantitative electron probe microanalysis of microscopical particles. *X-ray Spectrometry*, 20: 51–62.
- Wang R Z, Ripley E A, 1997. Effects of grazing on a *Leymus chinensis* grassland on the Songnen plain of northeastern China. *Journal of Arid Environments*, 36: 307–318.
- Wang Y, Zhuang G S, Tang A H, Zhang W J, Sun Y L, Wang Z F, An Z S, 2007. The evolution of chemical components of aerosols at five monitoring sites of China during dust storms. *Atmospheric Environment*, 41: 1091–1106.
- Wedepohl K H, 1995. The composition of the continental crust. *Geochimica et Cosmochimica Acta*, 59: 1217–1239.
- Zhang X Y, Arimoto R, An Z S, 1997. Dust emission from Chinese desert sources linked to variations in atmospheric circulation. *Journal of Geophysical Research*, 102(D23): 28041–28047.
- Zhang X Y, Arimoto R, An Z S, Cao J J, Wang D, 2001. Atmospheric dust aerosol over the Tibetan Plateau. *Journal of Geophysical Research*, 106(D16): 18471–18476.
- Zhang X Y, Gong S L, Arimoto R, Shen Z X, Mei F M, Wang D, Cheng Y, 2003. Characterization and temporal variation of Asian dust aerosol from a site in the Northern Chinese deserts. *Journal of Atmospheric Chemistry*, 58: 55–68.
- Zhang R J, Fu C B, Han Z W, Zhu C S, 2008. Characteristics of elemental composition of PM_{2.5} in the spring period at Tongyu in the semi-arid region of Northeast China. *Advances in Atmospheric Sciences*, 25(6): 922–931.
- Zheng X, Lv Y, 1995. Formation and evolution environment of Dabusu alkaline lake. *Journal of Salt Lake Science*, 3(4): 10–17.
- Zhu T C, 1993. Grasslands of China. In: Natural Grasslands-Eastern Hemisphere and Resume, Volume 8B, Ecosystems of the World (Coupland R T, ed.). Amsterdam: Elsevier. 61–82.
- Zhuang G S, Yi Z, Duce R A, Brown P R, 1992. Link between iron and sulphur cycles suggested by detection of Fe(II) in remote marine aerosols. *Nature*, 355: 537–539.